ELSEVIER

Neuropsychologia 43 (2005) 1060–1071

NEUROPSYCHOLOGIA

www.elsevier.com/locate/neuropsychologia

Activation in the MT-complex during visual perception of apparent motion and temporal succession

Axel Larsen[a,*], Søren Kyllingsbæk[a], Ian Law[b], Claus Bundesen[a]

[a] *Center for Visual Cognition, Department of Psychology, University of Copenhagen, Njalsgade 90, DK-2300 Copenhagen S, Denmark*
[b] *Neurobiology Research Unit, N9201, and PET and Cyclotron Unit, KF 3982, The Copenhagen University Hospital, Rigshospitalet, Denmark*

Received 11 December 2003; received in revised form 10 June 2004; accepted 6 October 2004

Abstract

Previous studies have shown that MT (i.e., the MT-complex) is activated during visual perception of apparent motion. To further explore the function of MT, we measured activation in MT by positron emission tomography (PET) using a broad range of stroboscopic stimulus events in which (a) the frame rate was so fast that observers perceived stimulus frames as simultaneous, (b) the frame rate was slower and generated compelling impressions of apparent motion, or (c) the frame rate was so slow that observers perceived temporal succession (successive views of the same objects at different locations) instead of motion. As expected, the simultaneity condition showed no activation (reliable increase in regional cerebral blood flow, rCBF) in MT whereas the motion condition showed activation in both left and right MT. However, the succession condition showed even stronger activation in left and right MT than did the motion condition. MT seems implicated in perception of retinal stimuli as successive views of the same object at different locations whether or not the views are connected by apparent motion.

Keywords: MT-complex; PET; Apparent motion

1. Introduction

A stationary stimulus object displayed successively in two different spatial positions may generate a compelling illusion of one object moving along the shortest path connecting the two positions. The spatiotemporal relations between the stimuli are critical for the perception of apparent motion. If the temporal separation is too short for a given spatial separation, observers perceive a pair of simultaneous, stationary stimuli, and if the temporal separation is too long, observers perceive temporal succession but no visual motion.

Systematic psychophysical studies of the spatiotemporal principles governing perceptual illusions of motion created by stroboscopic stimuli began with Wertheimer's (1912) pioneering work on motion perception. Extending Wertheimer's work, Korte (1915) formulated an empirical generalization later known as Korte's (1915) third law. Korte's third law states that the interstimulus interval required for apparent translatory motion is directly related to the distance between stimulus positions provided that stimulus exposure duration and intensity are kept constant.

Korte's third law is not valid as it stands (Caelli & Finlay, 1981; Kolers, 1972). However, later research (Caelli & Finlay, 1981; Corbin, 1942; Larsen, Farrell, & Bundesen, 1983) has supported a related conjecture by which the minimum temporal interval between the onsets of the successive stimuli (the stimulus-onset asynchrony or SOA) at the threshold of simultaneity, where the visual impression of a single object in smooth motion breaks down (cf. Corbin, 1942; Woodworth & Schlosberg, 1954), is a linearly increasing function of the spatial separation between the stimuli for separations above 1.5° (long-range apparent motion; for analogous results on apparent rotational motion, see Bundesen, Larsen, & Farrell, 1983; Farrell, Larsen, & Bundesen, 1982; Shepard & Judd, 1976).

Brain imaging studies using positron emission tomography (PET) (Taylor et al., 2000; Watson et al., 1993) or

* Corresponding author. Tel.: +45 3532 8812; fax: +45 3532 8682.
E-mail address: axel@psy.ku.dk (A. Larsen).

0028-3932/$ – see front matter © 2004 Elsevier Ltd. All rights reserved.
doi:10.1016/j.neuropsychologia.2004.10.011

functional magnetic resonance imaging (fMRI) (Morrone, Tosetti, Montarano, Fiorentini, Cioni, & Burr, 2000; Tootell et al., 1995a) have localized the human homolog of the highly motion responsive visual area V5 in the macaque monkey at a small area (MT) near the junction of the occipital, temporal, and parietal lobes. The exact location at which MT-activity peaks varies from one study to the next. To our knowledge, all reported MT-positions lie within a sphere with a radius of 12 mm approximately located at (±46, −68, 3) in classical Talairach space (Talairach & Tournoux, 1988); in the MNI-SPM96 implementation of the stereotactic atlas of Talairach and Tournoux (1988), the corresponding location is (±46, −70, 0). As suggested by Zeki and collaborators (Zeki et al., 1991) and confirmed in numerous later brain mapping studies (see e.g., Chawla et al., 1998; Cornette et al., 1998; Heeger, Boynton, Demb, Seidemann, & Newsome, 1999; Kaneoke, Bundou, Koyama, Suzuki, & Kakigi, 1997; Schenk & Zihl, 1997; Smith, Greenlee, Singh, Kraemer, & Hennig, 1998; Tootell et al., 1995a; Zeki & Ffytche, 1998), the MT-complex is strongly involved in motion processing.

MT appears to be assisted by other areas of the brain in the interpretation of visual motion. For example, sequential presentation of a square and a circle may create impressions of elastic motion (Zhuo et al., 2003), which seems to implicate shape-processing systems in the ventral pathways. Isoluminant higher-order motion stimuli have been shown to invoke V3 (Wenderoth, Watson, Egan, Tochon-Danguy, & O'Keefe, 1999) and in some cases the inferior parietal lobule (Claeys, Lindsey, De Schutter, & Orban, 2002). MT is also active when subjects experience motion aftereffects in the absence of stroboscopic stimulation (Taylor et al., 2000; Tootell et al., 1995b), or when motion is implied or may be inferred from static stimuli (Kourtzi & Kanwisher, 2000). Intentionally imagining visually perceived motion (Goebel, Khorram-Sefat, Muchli, Hacker, & Singer, 1998) or performing tasks in which visual images are mentally rotated (Alivisatos & Petrides, 1997; Cohen et al., 1996) or mentally moved in depth (changed in size; Larsen, Bundesen, Kyllingsbæk, Paulson, & Law, 2000) also seem to implicate the MT-complex.

In this article we examine visual processing of spatially translated luminance-defined stimuli (white bars on a black background) as a function of stimulus-onset asynchrony with PET. The spatial separation between stimuli in successive frames was fairly large (0.9°). This type of visual stimulation should bypass low level motion energy filters of the type envisaged by Adelson and Bergen (1985) and others and should predominantly capture long-range motion mechanisms (Anstis, 1980; Braddick, 1980; Larsen et al., 1983). Due to the special role of MT in visual motion processing,[1] we wanted to map the regional cerebral blood flow (rCBF) response in the MT-complex in the three phenomenally distinct states that may result from perceiving stroboscopic stimulation. Namely, when stroboscopic stimuli are displayed so close to each other in time that they are perceived as simultaneous with concurrent onsets and offsets and no impression of motion; when the flashing stimuli satisfy the spatiotemporal constraints specified in modern versions of Korte's third law and cause compelling illusory sensations of one stimulus moving from one location to another; and finally, when the onset and offset of a stimulus in one location is followed so slowly by the onset and offset of an identical stimulus in another location that there is no phenomenal experience of visual apparent motion.

It is a common procedure in psychophysical investigations of apparent motion to present two stimuli in a regular sequential alternation. With fixed stimulus exposure durations and different SOAs in the three experimental conditions, this procedure would lead to unequal numbers (frequencies) of simultaneity, motion, and slow succession events during a scan. Because intensity of brain activations estimated by PET or fMRI is highly correlated with frequency of stimulus events (cf. Fox & Raichle, 1984, 1985; Fox et al., 2000; Kaufmann, Elbel, Gossl, Putz, & Auer, 2001; Law, Jensen, Holm, Nickles, & Paulson, 2001; Mentis et al., 1997; Thomas & Menon, 1998; Zhu et al., 1998), we adopted a procedure in which the frequency of experimental events was the same in every scan. Pilot investigations suggested that a frequency of 0.25 Hz (corresponding to an inter-event interval of 4000 ms) was a good choice; this rate was high enough to be detectable by PET and slow enough to display two stimuli in succession without any visual impression of motion.

2. Method

2.1. Subjects

Eight right-handed subjects (four males, four females, mean age: 23.9 years, range: 22–27) were paid to participate. The study was approved by the local ethics committee of Copenhagen (J.nr. (KF) 01-339/94), and participants gave their informed written consent according to the Declaration of Helsinki II.

2.2. Stimuli

In order to increase the sensitivity of our method, we used large stimulus displays containing many high-contrast stimulus objects. Each stimulus frame contained 12 identical white rectangles each of which subtended 0.5° horizontally and 0.8° vertically (see Fig. 1). The rectangles were drawn on the black face of a computer-driven cathode-ray tube (CRT) and were displayed in three approximately equidistant rows and four approximately equidistant columns, with two columns to the left of the center of the screen and two columns to the right. The whole display subtended approximately 21°

[1] The spatial resolution of current PET technology does not allow precisely locating area MT or MST. In view of this limitation we only claim that our data describe activations in the MT-complex, that is, in or near areas MT and MST.

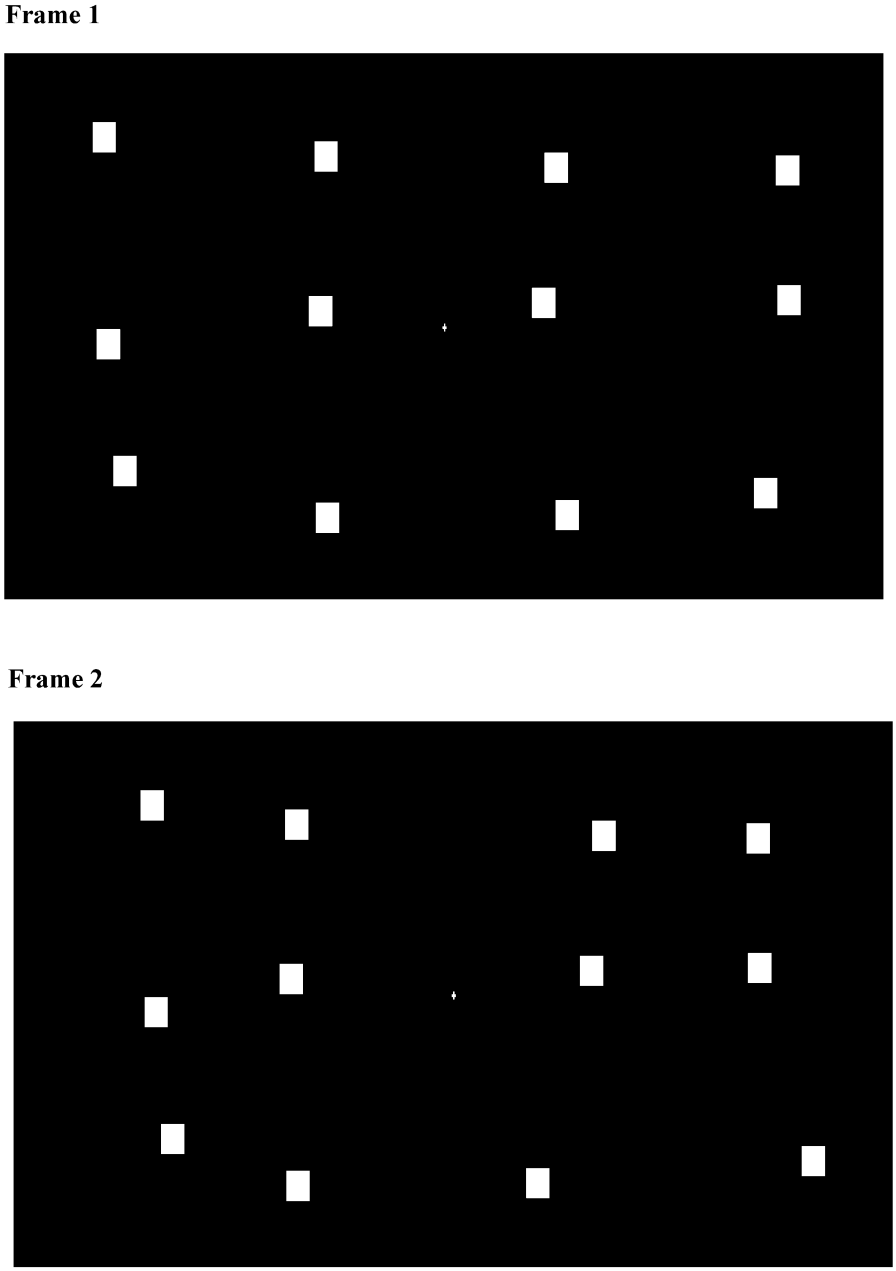

Fig. 1. Examples of the stroboscopic stimulus arrays used in the experiment. In the stationary and in the simultaneity condition the two arrays were superimposed. In motion and succession conditions only one stimulus array was displayed at a time.

horizontally and 14° vertically. The global three by four matrix of rectangle positions was fixed. However, to avoid adaptation, the precise positions of the rectangles in the stimulus display were varied slightly from trial to trial by shifting the individual rectangles independently up or down and left or right by up to 0.3° of visual angle.

2.3. Design

The subjects were PET scanned in three experimental conditions and two control conditions. In the fixation cross control condition (two scans) the stimulus display was empty (black) except for the white five-pixel cross in the center, which was displayed in all scan conditions. The stationary control condition (one scan) showed the two superimposed stimulus frames (a total of 24 rectangles) throughout the scan. The first stimulus array was constructed as indicated above and the second array was identical to the first, except that each rectangle was shifted to the left or to the right by 0.9° as determined by a random draw with a probability of 0.5.

The three experimental conditions were identical except as noted below and always showed two three-by-four matrices of small rectangles, each for a duration of 83 ms, followed by the same two stimulus frames after a trial-onset asynchrony

of 4000 ms. In the simultaneity condition (three scans), we first attempted to set SOA between first and second stimulus frame to a value greater than 0 ms. However, even with an SOA of 16.67 ms (due to the screen refresh rate of 60 Hz, the lowest possible increment of SOA) a few subjects sometimes had impressions of (rapid) motion. Accordingly, in the simultaneity condition, SOA was fixed at 0 ms such that the two stimulus frames were superimposed, showing a total of 24 rectangles for 83 ms once every 4000 ms. In the motion condition (three scans) SOA was 83 ms, and in the succession condition (three scans) SOA was 1667 ms. Thus, the three experimental conditions were identical with regards to both numbers of physical onsets and offsets of white rectangles and total amount of luminous energy during the scans. The design and the five conditions are displayed graphically in Fig. 2.

2.4. Procedure

Each subject received 12 scans, which were divided into three blocks of four scans. Each block comprised one of each of the three experimental conditions and one control condition. The sequence of blocks and the sequence of conditions within blocks were randomized anew for each participant.

The participants were instructed to keep fixation at the small cross in the center of the display screen during the scanning sessions, which were initiated approximately 30 s

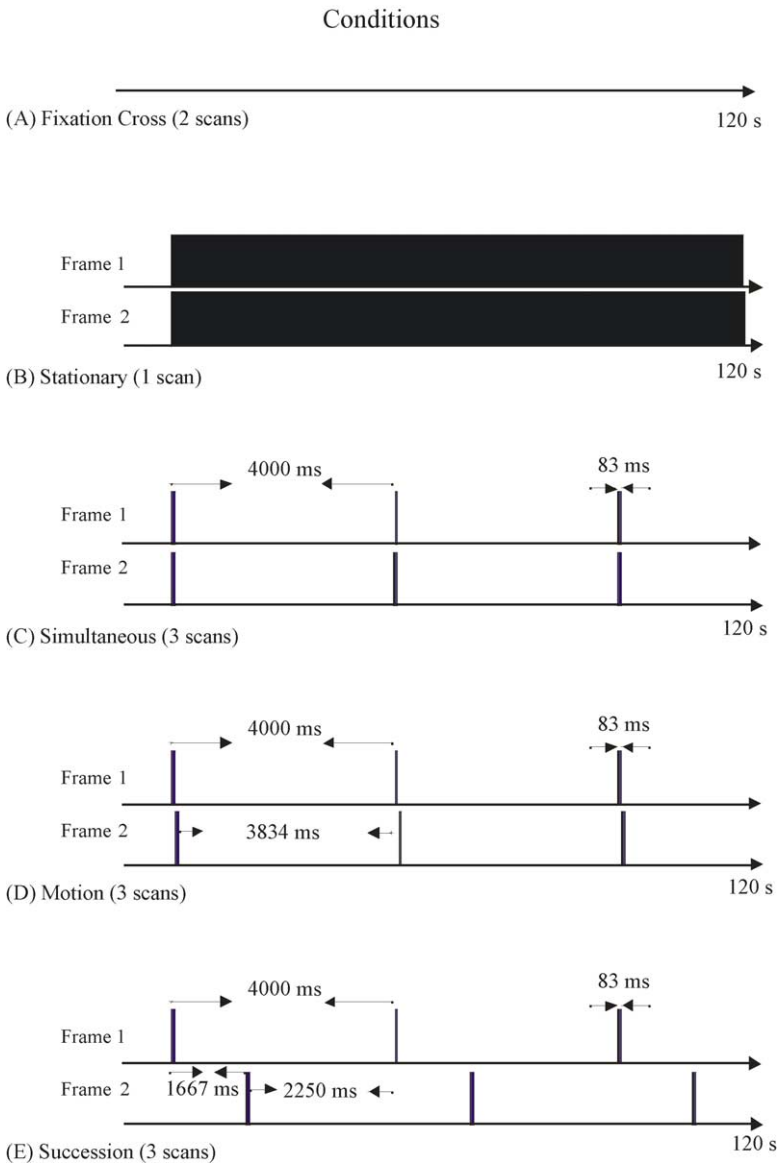

Fig. 2. Graphical display of experimental conditions. All conditions lasted for about 120 s, during which subjects were instructed to keep fixation at a small cross in the center of the stimulus display. Onsets and exposure durations of the two stimulus frames are indicated by black bars on the time axes. Stimulus-onset asynchronies, interstimulus intervals, and intertrial intervals can be read off from the display.

prior to isotope arrival to the brain and continued during the 90 s acquisition period. Interscan interval was 10 min.

PET scans were obtained with an 18-ring GE-Advance scanner (General Electric Medical Systems, Milwaukee, WI, USA) operating in 3D acquisition mode, producing 35 image slices with an interslice distance of 4.25 mm. The total axial field of view was 15.2 cm with an approximate in-plane resolution of 5 mm. The technical specifications have been described elsewhere (DeGrado et al., 1994).

For each scan the subject received a slow intravenous bolus injection of 400 MBq (10.8 mCi) of $H_2{}^{15}O$. The isotope was administered via an antecubital intravenous catheter over 30 s by an automatic injection device. Head movements were limited by head-holders constructed by thermally moulded foam. Before the activation sessions a 10 min transmission scan was performed for attenuation correction. Images were reconstructed with a 4.0 mm Hanning filter transaxially and an 8.5 mm Ramp filter axially. The resulting distribution images of time-integrated counts were used as indirect measurements of the regional neural activity.

2.5. Image analysis

For all subjects the complete brain volume was sampled. Image analysis was performed using Statistical Parametric Mapping software (SPM-96, Wellcome Department of Cognitive Neurology, London, UK; Frackowiak & Friston, 1994). All intrasubject images were aligned on a voxel-by-voxel basis using a 3D automated six-parameters rigid body transformation (AIR 3.0; Woods, Cherry, & Mazziotta, 1992), and anatomical MRI scans were co-registered to the individual averages of the 12 aligned PET scans. The average PET scans and corresponding anatomical MRI scans were subsequently transformed into the standard stereotactic atlas of Talairach and Tournoux (1988) using the PET template defined by the Montreal Neurological Institute (MNI; Friston et al., 1995a). The stereotactically normalized images consisted of 68 planes of 2 mm × 2 mm × 2 mm voxels. Before statistical analysis, images were filtered by a 16 mm (FWHM) isotropic Gaussian filter to increase the signal-to-noise ratio and to accommodate residual variability in morphological and topographical anatomy that was not accounted for by the stereotactic normalization process (Friston, 1994). Differences in global activity were removed by proportional normalization to a value of 50. Only intracerebral areas that did not change significantly ($p > 0.05$) between conditions were selected to represent global activity following the iterative approach described by Andersson (1997).

Analyses were performed over the whole brain volume and in a region of interest (ROI) consisting of two spheres with 12 mm radii centered at (±46, −70, 0) in the MNI-SPM96 implementation of the stereotactic space defined by Talairach and Tournoux (1988). The two spheres are centered close to and includes the MT/V5 locations (−47, −76, 2) and (44, −67, 0) estimated in the detailed study of 19 hemispheres by Dumoulin et al. (2000). Our ROI also agrees closely with the results of the Brede database metaanalysis of 8 published studies (Nielsen & Hansen, 2002) in which the average location of left and right MT was (−49, −70, 3) and (46, −67, 1), respectively.

The ROI volumes were extracted by in-house software and kept in the space of the standard stereotactic atlas of Talairach and Tournoux (1988) using the MNI PET template. Whole brain as well ROI volumes were processed by the SPM96 software which in either case tested the null hypothesis of no regionally specific activation effects of the experimental conditions by comparing conditions on a voxel-by-voxel basis. The resulting set of voxel values constituted a statistical parametric map of the *t*-statistic, SPM$\{t\}$. A transformation of values from the SPM$\{t\}$ into the unit Gaussian distribution using a probability integral transform allowed changes to be reported in *Z*-scores (SPM$\{Z\}$). Voxels were considered significant if their *Z*-score exceeded a threshold of $p < 0.05$ after correction for multiple non-independent comparisons. This threshold was estimated according to Friston, Frith, Liddle, and Frackowiak (1991) and Friston et al. (1995b) using the theory of Gaussian fields. The resulting foci were then characterized in terms of peak *Z*-score above this level. Anatomical locations are indexed by the measures established in the MNI-SPM96 implementation of the stereotactic atlas of Talairach and Tournoux (1988).

2.6. Supplementary study

To obtain supplementary behavioral evidence on the visual appearance of the stimuli in the three experimental conditions, we asked 10 new participants (students or members of staff who were naive with respect to the purpose of the experiment) to describe the visual appearance of the stimuli in words and subsequently rate their visual impressions of motion on a 7-point scale ranging from no impression of motion (rating = 1) to strongest possible impression of motion (rating = 7, implying that the apparent motion was indistinguishable from real motion). These new observers were tested individually in a semi-darkened experimental laboratory sitting 60 cm in front of the display screen. Viewing conditions were otherwise the same as the viewing conditions in the scanner.

3. Results

3.1. Behavioral data

3.1.1. Main experiment

All subjects reported that an array of white bars appeared to flash on and off at fixed time intervals in the simultaneity condition whereas the two stimulus frames appeared in slow sequential alternation in the succession condition. When questioned they gave no reports of impressions of motion in these conditions. In the motion condition they reported (in agreement with the composition of the stroboscopic stimulus

displays) that a group of bars appeared briefly at fixed time intervals and that some of the bars moved to the right and the remaining ones to the left.

3.1.2. Supplementary study

None of the 10 participants in the supplementary study reported any impression of visual motion in the simultaneity condition (mean rating = 1.0). In the succession condition, three of the participants reported weak impressions of visual motion (ratings of 2 and 3) but seven participants reported perceived succession without any impression of visual motion (ratings of 1, yielding an overall mean rating of 1.5 for the succession condition). By contrast, in the motion condition, all 10 participants reported visual impressions of motion (mean rating = 4.7, range 3–6).

The participants' verbal descriptions of the visual appearance of the stimuli indicated that in both the motion condition and the succession condition, each rectangle in the first stimulus frame was grouped with the corresponding rectangle in the second stimulus frame so that the two rectangles were perceived as successive views of the same object at different locations. The two views were connected by apparent motion in the motion condition, but the views were generally not connected by apparent motion in the succession condition.

3.2. PET data

Our principal interest was to map the MT activity in the predefined, bilateral region of interest as a function of the spatiotemporal variation of the stimulus arrays. For completeness we also describe and graphically illustrate whole-brain statistical parametic maps.

3.2.1. Simultaneity condition

In this condition the two stimulus frames were concurrently presented (superimposed with SOA = 0 ms) for 83 ms every 4000 ms (i.e. a stimulus event frequency of 0.25 Hz) during the scan. Measured by the contrast to the fixation cross condition or the stationary condition, there were no measurable effects of the simultaneous stimulus presentation within the bilateral region of interest, which included MT. In the comparisons with the two control conditions in the whole-brain analysis, the only statistically reliable effect was the simultaneity–fixation cross contrast, which is shown in Fig. 3A and Table 1. There was reliable activity in voxels in or close to left and right primary cortex (BA 17, BA 18).

3.2.2. Motion condition

The motion condition was identical to the simultaneity condition except that SOA between stimulus frames

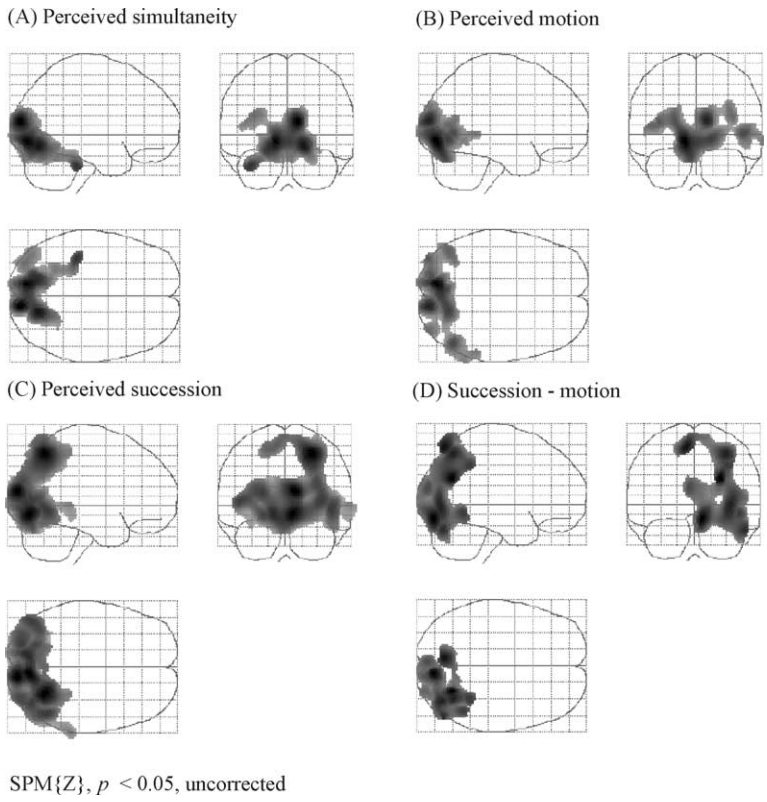

Fig. 3. Maximum intensity statistical parametric map (SPM{Z}> 1.65, $p < 0.05$, uncorrected) projections of the contrast between the three experimental conditions and the fixation cross control condition (panels A, B, and C). Panel D shows the contrast between succession and motion. Left on figure is left on brain.

Table 1
rCBF during perceived simultaneity, motion, and succession

Anatomical structure	Region *K*	Talairach coordinates			Voxel *Z*-score	ΔrCBF (%)	*p*
		x	*y*	*z*			
Simultaneity–fixation cross contrast: whole brain							
Cuneus, BA 17/18 (R)	8202	10	−90	14	4.55	3.10	0.024
Lingual gyrus, BA 17/18 (L)		−12	−82	−6	4.46	2.79	0.035
Motion–fixation cross contrast: ROI analysis							
Middle temporal gyrus, MT (R)	496	50	−66	2	3.14	1.97	0.016
Middle temporal gyrus, MT (L)	255	−44	−68	10	2.70	1.61	0.042
Motion–stationary contrast: ROI analysis							
Middle temporal gyrus, MT (R)	179	56	−66	8	2.87	2.31	0.032
Motion–fixation cross contrast: whole brain							
Lingual gyrus, BA 17/18 (L)	7355	−12	−82	−6	4.39	2.74	0.046
Succession–fixation cross contrast: ROI analysis							
Middle temporal gyrus, Anterior MT (R)	1083	48	−60	−4	4.10	3.02	0.001
Middle occipital/middle temporal gyrus, MT (R)		38	−76	6	4.07	2.87	0.001
Middle occipital/middle temporal gyrus, MT (L)	622	−46	−76	4	3.99	2.78	0.001
Succession–stationary contrast: ROI analysis							
Middle temporal gyrus, MT (R)	377	50	−72	10	3.19	2.60	0.014
Succession–fixation cross contrast: whole brain							
Cuneus, BA 18 (R)	18271	10	−90	16	5.21	3.62	0.001
Superior parietal lobule, BA 7 (R)		28	−62	54	5.18	5.04	0.001
Lingual gyrus, BA 18 (R)		8	−78	−8	5.14	3.38	0.002

Note: ROI, two spheres with radii of 12 mm centered at (±46, −70, 0). The first column tabulates the set of *K* activated voxels ($Z > 1.65$, $p < 0.05$, uncorrected). Within each region, the anatomical location of the voxel with the maximum *Z*-score is indexed by the measures established in the MNI-SPM96 implementation of the stereotactic atlas of Talairach and Tournoux (1988). Negative *x*-coordinates indicate left-hemisphere locations. All levels of significance are corrected for multiple comparisons.

alternated between 83 and 3917 ms (Fig. 2). In the ROI analysis (Table 1), the motion–fixation cross contrast showed significantly activated regions with activity peaks in the left and right hemisphere MT; there was also a significant region with a peak in the right hemisphere MT in the motion–stationary contrast. The results of the whole-brain analysis of the motion–fixation cross contrast are shown in Fig. 3B and Table 1. Only a few voxels were reliably activated in the occipital cortex. The motion–stationary contrast did not reach significance.

3.2.3. Succession condition

In this condition the SOA between stimulus frames alternated between 1667 and 2333 ms (Fig. 2), but otherwise the condition was identical to the motion and simultaneity conditions. The ROI analysis of the contrast between the succession and fixation cross conditions (Table 1) showed activated regions with peaks in left and right hemisphere MT, while the contrast to the stationary condition only revealed activity in right MT. In the whole-brain analysis the contrast to the fixation cross condition (Fig. 3C and Table 1) showed extensive activations in a region predominantly covering occipital visual areas (BA 18) and the parietal cortex (BA 7) in the right hemisphere. There were no reliable activations by the contrast to the stationary condition.

3.2.4. Comparing perceived stimulus succession with perceived motion

Fig. 3D shows the whole-brain statistical parametric map of the contrast between succession and motion, and Fig. 4 shows the map rendered in 3D. Note that the data in Figs. 3 and 4 are uncorrected for multiple comparisons. The results of the ROI analysis are reported in Table 2. As can be seen, rCBF in left and right hemisphere MT and adjacent areas was significantly higher in the succession condition than in the motion condition.

4. Discussion

We interpret our data on the general assumption that rCBF estimated by PET is monotonically related to neural activity. We also base our analyses on the fact that the three experimental conditions were identical except for the relative timings of the first and second stimulus frames. Numbers of stimulus onsets and offsets and total luminous energy were exactly the same in the three conditions (cf. Fig. 2).

4.1. Simultaneity

In the simultaneity condition, in which stimulus arrays were presented at the same time with a repetition frequency of

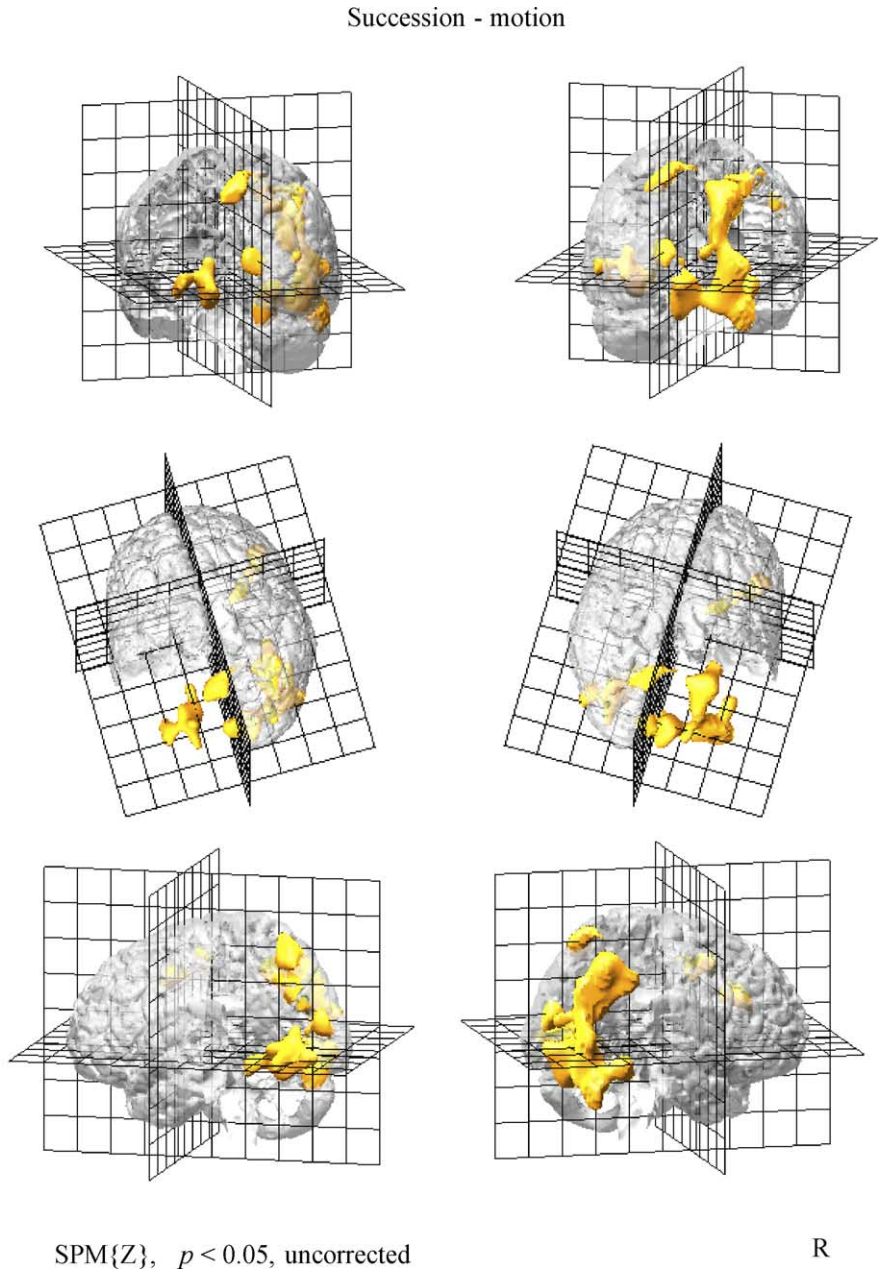

Fig. 4. Maximum intensity 3D statistical parametric maps (SPM{*Z*}> 1.65, $p < 0.05$, uncorrected) of the contrast between succession and motion conditions. Left on figure is left on brain.

Table 2
Comparison of rCBF in succession and motion conditions: ROI analysis

Anatomical structure	Region *K*	Talairach coordinates			Voxel *Z*-score	ΔCBF (%)	*p*
		x	*y*	*z*			
Succession–motion contrast							
Middle occipital/inferior temporal gyrus, MT (R)	676	36	−76	−2	3.16	2.13	0.015
Middle occipital/middle temporal gyrus, MT (R)		42	−78	4	2.87	1.76	0.030
Middle occipital/middle temporal gyrus, MT (L)	429	−46	−80	4	2.67	1.81	0.044

Note: ROI, two spheres with radii of 12 mm centered at (±46, −70, 0). The first column tabulates the set of *K* activated voxels ($Z > 1.65$, $p < 0.05$, uncorrected). Within each region, the anatomical location of the voxel with the maximum *Z*-score is indexed by the measures established in the MNI-SPM96 implementation of the stereotactic atlas of Talairach and Tournoux (1988). Negative *x*-coordinates indicate left-hemisphere locations. All levels of significance are corrected for multiple comparisons.

0.25 Hz, we found increased activity with peaks in or close to primary visual cortex, but no measurable activation in the region of interest that included MT. The results extend previous research on the effects of visual stimulus presentation rate on brain activation measured by PET or fMRI (Fox & Raichle, 1984, 1985; Fox et al., 2000; Kaufmann et al., 2001; Law et al., 2001; Mentis et al., 1997; Ozus et al., 2001; Thomas & Menon, 1998; Zhu et al., 1998). These studies showed that repetitive stimulus events with frequencies above 0.5 Hz generate activation in primary visual cortex and neighboring areas with the maximum activation obtained at frequencies in the range between 6 and 15 Hz.

4.2. Succession

When the temporal displacement between stimulus frames was increased up to 1667 ms, all subjects in the main experiment and 7 out of 10 subjects in the supplementary study reported that they perceived temporal succession (first Frame 1, then Frame 2) without any impression of visual motion. Participants also reported that each rectangle in the first stimulus frame was grouped with the corresponding rectangle in the second stimulus frame so that the two rectangles were perceived as successive views of the same object at different locations. Table 1 and Figs. 3 and 4 show right hemisphere increases in rCBF in the parietal (BA 7) and the occipital (BA 18) cortex. Corrected for multiple comparisons there was no reliable activation of BA 17 (striate visual cortex). Adding the results from the ROI analysis (Table 2), the data suggest that MT is implicated in perception of retinal images as successive views of the same object at different locations regardless of whether the views are connected by apparent motion. In fact, the activation in MT was stronger in the succession condition (in which subjects perceived little or no apparent motion) than in the motion condition (in which subjects perceived fairly strong apparent motion) (see Table 2 and Fig. 3D).

The spatiotemporal boundaries (or window) within which MT is active are not well known. Studies on rate dependent activation in visual cortical areas (see Fox & Raichle, 1984, 1985; Fox et al., 2000; Kaufmann et al., 2001; Law et al., 2001; Mentis et al., 1997; Ozus et al., 2001; Thomas & Menon, 1998; Zhu et al., 1998) suggest that the window has a lower spatial limit greater than 0° of visual angle. In these studies, in which the visual stimulus events were repeated at the same location, there was no response in MT unless there was some spatial displacement from one stimulus frame to the next.[2] Correspondingly, one might ask whether there are upper limits to the spatial and temporal separations between stimuli that can activate MT. More generally, how are the spatiotemporal conditions for MT activation? An extensive parametric study of these conditions might show substantial resemblance to the spatiotemporal constraints embodied in Korte's third law for apparent motion. Obviously, our data on this issue are sparse. They indicate that successive presentations of the same stimulus separated by 0.9° of visual angle elicit neural signals in MT when SOA ranges from 83 ms up to at least 1667 ms.

4.3. Motion

In the motion condition, subjects reported that short bursts of rapidly moving rectangles were recurrently displayed, and in agreement with expectations rCBF increased within the region of interest in locations that can be identified with MT. The data from the supplementary study (average rating 4.7) indicate that the impression of motion was fairly strong although the apparent motion was distinguishable from real motion. As can be seen from Table 1, the loci of peak intensity in the hypothesized MT region established by the contrast between the motion and fixation cross conditions are in good agreement with, though slightly anterior to, previous brain mappings of MT (e.g., [45/50, −76/−82, 3/−1] in classical Talairach space and [42/47, −69/−75, 0/−4] in the MNI-SPM96 implementation of Talairach space; cf. Tootell et al., 1995a; Watson et al., 1993). The contrast to the stationary condition, by which processing in early visual areas common to many visual tasks (including motion) is subtracted, revealed a peak activity confined to the right hemisphere MT (56, −66, 8).

Disregarding activation in MT, rCBF was generally similar during asynchronous (motion) and simultaneous presentation of stimulus frames (see Fig. 3). Very much the same pattern of results was reported by Muckli et al. (2002) in an event related fMRI study with a bistable stroboscopic stimulus that was sometimes perceived as flashing on and off and sometimes as rapidly moving back and forth between two locations in visual space. Overall our findings agree well with previous work and support the claim that neural processing in MT is critical for luminance-defined motion perception.

The whole-brain analysis of our data from the motion condition also showed increased rCBF in left BA 17/18 and presumably parts of primary visual cortex. These data are broadly consistent with findings from many brain mapping studies on visual motion using PET or fMRI (see e.g., Chawla et al., 1998; Cornette et al., 1998; Heeger et al., 1999; Kaneoke et al., 1997; Morrone et al., 2000; Muckli et al., 2002; Schenk & Zihl, 1997; Smith et al., 1998; Taylor et al., 2000; Tootell et al., 1995a; Vanduffel et al., 2002; Watson et al., 1993; Zeki & Ffytche, 1998; Zeki et al., 1991).

4.4. Theoretical interpretation

Perception of long-range apparent motion may require several stages of processing. In one theory (Ullman, 1979; also see Bundesen, 1989; Bundesen et al., 1983), three stages

[2] In studies of visual rate dependence it is fairly common to use annular reversing checkerboard patterns. The reversing fields may be perceived as flicker without change of position. However, if the timing is right, individual stimulus fields may be perceptually interpreted to move and shift position (see, e.g., Kaufmann et al., 2001; Law et al., 2001).

are required. Given two successive images of a scene that are separated in space and time, the visual system first identifies corresponding parts of the two images. For example, given Stimulus Frames 1 and 2, the visual system groups each rectangle in Frame 1 together with the corresponding rectangle in Frame 2 as successive views of the same object at different locations. Second, when the "correspondence problem" has been solved, the system computes the motion intervening between the two presentations. Finally, for each pair of corresponding rectangles, the computed trajectory is *impleted* (Beck et al., 1977) or "filled in" by generation of a sequence of visual representations of the object in successive positions along the path from the position indicated by the first image to the position indicated by the second one—a sequence of representations similar to those that would have been generated if the object had been viewed in real motion over the trajectory.

In terms of the three-stage theory, our findings may be explained by assuming that the strength of MT activation reflected the amount of neural computation required to solve the correspondence problem and compute the motion intervening between the presentations of Frames 1 and 2 without impleting the computed trajectories. These two stages of processing should be completed in both the motion and the succession conditions, and the amount of computation needed to complete the stages may have been somewhat greater in the succession condition because the correspondence must be established across a longer temporal separation. The impletion process underlying the visual impression of apparent motion should be found in the motion condition but not in the succession condition. By the suggested explanation of our findings, the impletion process occurs in the network of visual areas with which MT is reciprocally connected (see DeYoe & Van Essen, 1988; Shipp & Zeki, 1989) rather than occurring in MT itself.[3]

5. Conclusion

In this PET investigation our principal goal was to map activity in the MT-complex in perception of visual simultaneity, apparent motion, and temporal succession. This was done by varying the locations and the stimulus-onset asynchrony of successively displayed arrays of white bars. There were three experimental conditions in which each of two stimulus arrays was presented for 83 ms every 4000 ms. The stimulus-onset asynchrony was 0 ms in the simultaneity condition, 83 ms in the motion condition, and 1667 ms in the succession condition, and the spatial separation (0.9°) between corresponding elements in the stroboscopic displays was judged large enough for bypassing low level motion filters and activating long-range motion mechanisms. There were two baseline conditions, in which the stimulation was kept constant throughout the scan. In one of the baseline conditions, only the fixation cross was displayed; in the other one, the two stimulus arrays were superimposed upon each other. Compared with these baselines, the simultaneity condition showed no activation in MT, whereas the motion condition showed strong activation in MT. However, the succession condition showed even stronger activation in MT than did the motion condition. The data suggest that MT is implicated in perception of retinal images as successive views of the same object at different locations regardless of whether the views are connected by apparent motion. The data may be explained by assuming that MT is implicated in solving the correspondence problem and computing the trajectories of long-range apparent motion whereas the impletion (filling in) process underlying the visual impression of apparent motion occurs in the network of visual areas with which MT is reciprocally connected rather than occurring in MT itself.

[3] Extant evidence on the role of striate and low-level extrastriate cortical areas in long-range apparent motion is inconclusive. In ongoing fMRI experiments, we have obtained suggestive evidence of activation in V1 during perception of long-range apparent motion, though Liu, Slotnick, and Yantis (2004) reported negative findings. Data from cortically blind patients and recent findings with transcranial magnetic stimulation (Cowey & Walsh, 2000; Pascual-Leone & Walsh, 2001; see also the discussion in Blake, Sekuler, & Grossman, 2004) are consistent with the notion that long-range apparent motion is generated by backprojections from MT to lower-level visual areas. For further evidence on the role of V1 in visual experience of motion, see Azziopardi and Cowey (2001) and Zeki and Ffytche (1998).

Acknowledgements

This work was supported by grants from the Danish Research Council for the Humanities and the Carlsberg Foundation. We thank Claus Svarer and Karin Stahr for technical assistance and Olaf B. Paulson for generous support during all phases of the project. The John and Birthe Meyer Foundation is gratefully acknowledged for the donation of the Cyclotron and PET scanner.

References

Adelson, E. H., & Bergen, J. R. (1985). Spatiotemporal energy models for the perception of motion. *Journal of the Optical Society of America A, 2*, 284–299.

Alivisatos, B., & Petrides, M. (1997). Functional activation of the human brain during mental rotation. *Neuropsychologia, 35*, 111–118.

Andersson, J. L. (1997). How to estimate global activity independent of changes in local activity. *Neuroimage, 6*, 237–244.

Anstis, S. M. (1980). The perception of apparent movement. *Philosophical Transactions of the Royal Society of London B, 290*, 153–168.

Azziopardi, P., & Cowey, A. (2001). Motion discrimination in cortically blind patients. *Brain, 124*, 30–46.

Beck, J., Elsner, A., & Silverstein, C. (1977). Position uncertainty and the perception of apparent movement. *Perception & Psychophysics, 21*, 33–38.

Blake, R., Sekuler, R., & Grossman, E. (2004). Motion processing in the human visual cortex. In J. H. Kaas & C. E. Collins (Eds.), *The primate visual system* (pp. 311–344). Boca Raton, Florida: CRC Press.

Braddick, O. (1980). Low-level and high-level processes in apparent motion. *Philosophical Transactions of the Royal Society of London B, 290*, 137–151.

Bundesen, C. (1989). Spatio-temporal conditions for apparent movement. *Physica Scripta*, *39*, 128–132.

Bundesen, C., Larsen, A., & Farrell, J. E. (1983). Visual apparent movement: Transformations of size and orientation. *Perception*, *12*, 549–558.

Caelli, T., & Finlay, D. (1981). Intensity, spatial frequency, and temporal frequency determinants of apparent motion: Korte revisited. *Perception*, *10*, 183–189.

Chawla, D., Phillips, J., Buechel, C., Edwards, R., & Friston, K. J. (1998). Speed-dependent motion-sensitive responses in V5: an fMRI study. *Neuroimage*, *7*, 86–96.

Claeys, K. G., Lindsey, D. T., De Schutter, E., & Orban, G. A. (2002). Higher order motion in human inferior parietal lobule: Evidence from fMRI. *Neuron*, *40*, 631–642.

Cohen, M. S., Kosslyn, S. M., Breiter, H. C., DiGirolamo, G. J., Thompson, W. L., Anderson, A. K., Bookheimer, S. Y., Rosen, B. J., & Belliveau, J. (1996). Changes in cortical activity during mental rotation: A mapping study using functional MRI. *Brain*, *119*, 89–100.

Corbin, H. H. (1942). The perception of grouping and apparent movement in visual depth. *Archives of Psychology*, *273*, 1–50.

Cornette, L., Dupont, P., Spileers, W., Sunaert, S., Michiels, J., Van-Hecke, P., Mortelmans, L., & Orban, G. A. (1998). Human cerebral activity evoked by motion reversal and motion onset. *Brain*, *121*, 143–157.

Cowey, A., & Walsh, V. (2000). Magnetically induced phosphenes in sighted, blind, and blindsighted observers. *Neuroreport*, *11*, 1066.

DeGrado, T. R., Turkington, T. G., Williams, J. J., Stearns, C. W., Hoffman, J. M., & Coleman, R. E. (1994). Performance characteristics of a whole-body PET scanner. *Journal of Nuclear Medicine*, *35*, 1398–1406.

DeYoe, E. A., & Van Essen, D. C. (1988). Concurrent processing streams in the monkey visual cortex. *Trends in Neuroscience*, *11*, 219–226.

Dumoulin, S. O., Bittar, R. G., Kabani, N. J., Baker, C. L., Le Goualher, G., Pike, G. B., et al. (2000). A new anatomical landmark for reliable identification of human area V5/MT: A quantitative analysis of sulcal patterning. *Cerebral Cortex*, *10*, 454–463.

Farrell, J. E., Larsen, A., & Bundesen, C. (1982). Velocity constraints on apparent rotational movement. *Perception*, *11*, 541–546.

Fox, P. T., & Raichle, M. E. (1984). Stimulus rate dependence of regional cerebral blood flow in human striate cortex demonstrated by positron emission tomography. *Journal of Neurophysiology*, *51*, 1109–1120.

Fox, P. T., & Raichle, M. E. (1985). Stimulus rate determines regional brain blood flow in striate cortex. *Annual Review of Neurology*, *17*, 303–305.

Fox, P. T., Ingham, R. J., Ingham, J. C., Zamarripa, F., Xiong, J. H., & Lancaster, J. L. (2000). Brain correlates of stuttering and syllable production. A PET performance-correlation analysis. *Brain*, *123*, 1985–2004.

Frackowiak, R. S. J., & Friston, K. J. (1994). Functional neuroanatomy of the human brain: Positron emission tomography: A new neuroanatomical technique. *Journal of Anatomy*, *184*, 211–225.

Friston, K. J. (1994). Statistical parametric mapping. In R. Thatcher, M. Hallet, T. Zeffiro, J. E. Roy, & M. Huerta (Eds.), *Functional neuroimaging: Technical foundations* (pp. 79–94). San Diego: Academic Press.

Friston, K. J., Ashburner, J., Frith, C. D., Poline, J. B., Heather, J. D., & Frackowiak, R. S. J. (1995). Spatial registration and normalization of images. *Human Brain Mapping*, *2*, 165–189.

Friston, K. J., Frith, C. D., Liddle, P. F., & Frackowiak, R. S. (1991). Comparing functional (PET) images: The assessment of significant change. *Journal of Cerebral Blood Flow and Metabolism*, *11*, 690–699.

Friston, K. J., Holmes, A. P., Worsley, K. J., Poline, J. B., Frith, C. D., & Frackowiak, R. S. J. (1995). Statistical parametric maps in functional imaging: A general linear approach. *Human Brain Mapping*, *2*, 189–210.

Goebel, R., Khorram-Sefat, D., Muchli, L., Hacker, H., & Singer, W. (1998). The constructive nature of vision: Direct evidence from functional magnetic resonance imaging studies of apparent motion and motion imagery. *European Journal of Neuroscience*, *10*, 1563–1573.

Heeger, D. J., Boynton, G. M., Demb, J. B., Seidemann, E., & Newsome, W. M. (1999). Motion opponency in the visual cortex. *Journal of Neuroscience*, *19*, 7162–7174.

Kaneoke, Y., Bundou, M., Koyama, S., Suzuki, H., & Kakigi, R. (1997). Human cortical area responding to stimuli in apparent motion. *Neuroreport*, *8*, 677–682.

Kaufmann, C., Elbel, G. K., Gossl, C., Putz, B., & Auer, D. P. (2001). Frequency dependence and gender effects in visual cortical regions involved in temporal frequency dependent pattern processing. *Human Brain Mapping*, *14*, 28–38.

Kolers, P. (1972). *Aspects of motion perception*. Oxford: Pergamon Press.

Korte, A. (1915). Kinematoscopische Untersuchungen. *Zeitschrift für Psychologie*, *72*, 193–296.

Kourtzi, Z., & Kanwisher, N. (2000). Activation in human MT/MST by static images with implied motion. *Journal of Cognitive Neuroscience*, *12*, 48–55.

Larsen, A., Farrell, J. E., & Bundesen, C. (1983). Short- and long range processes in visual apparent movement. *Psychological Research*, *45*, 11–18.

Larsen, A., Bundesen, C., Kyllingsbæk, S., Paulson, O. B., & Law, I. (2000). Brain activation during mental transformation of size. *Journal of Cognitive Neuroscience*, *12*, 763–774.

Law, I., Jensen, M., Holm, S., Nickles, R. J., & Paulson, O. B. (2001). Using $^{10}CO_2$ for single subject characterization of the stimulus frequency dependence in visual cortex: A novel positron emission tomography tracer for human brain mapping. *Journal of Cerebral Blood Flow and Metabolism*, *21*, 1003–1012.

Liu, T., Slotnick, S. D., & Yantis, S. (2004). Human MT+ mediates perceptual filling-in during apparent motion. *Neuroimage*, *21*, 1772–1780.

Mentis, M. J., Alexander, G. E., Grady, C. L., Horwitz, B., Krasuski, J., Pietrini, P., et al. (1997). Frequency variation of a pattern-flash visual stimulus during PET differentially activates brain from striate through frontal cortex. *Neuroimage*, *5*, 116–128.

Morrone, M. C., Tosetti, M., Montarano, D., Fiorentini, A., Cioni, G., & Burr, D. C. (2000). A cortical area that responds specifically to optic flow, revealed by fMRI. *Nature Neuroscience*, *3*, 1322–1328.

Muckli, L., Kriegeskorte, N., Lanfermann, H., Zanella, F. E., Singer, W., & Goebel, R. (2002). Apparent motion: Event-related functional magnetic resonance imaging of perceptual switches and states. *The Journal of Neuroscience*, *22 RC219*, 1–5.

Nielsen, F.Å., Hansen, L.K. (2002). Automatic anatomical labeling of Talairach coordinates and generation of volumes of interest via the BrainMap database. In Proceedings of the Eight International Conference on Functional Mapping of the Human Brain, June 2–6, 2002, Sendai, Japan. *NeuroImage 16*(2) (Available on CD-Rom http://hendrix.imm.dtu.dk/services/jerne/brede/WOROI_103.html).

Ozus, B., Liu, H.-L., Chen, L., Meenakshi, B. I., Fox, P. T., & Gao, J.-H. (2001). Rate dependence of human visual cortical response due to brief stimulation: An event-related fMRI study. *Magnetic Resonance Imaging*, *19*, 21–25.

Pascual-Leone, A., & Walsh, V. (2001). Fast backprojections from the motion to the primary visual area necessary for visual awareness. *Science*, *292*, 510–512.

Schenk, T., & Zihl, J. (1997). Visual motion perception after brain damage: I. Deficits in global motion perception. *Neuropsychologia*, *35*, 1289–1297.

Shepard, R. N., & Judd, S. A. (1976). Perceptual illusion of rotation of three-dimensional objects. *Science*, *191*, 952–954.

Shipp, S., & Zeki, S. (1989). The organization of connections between areas V5 and V1 in macaque monkey visual cortex. *European Journal of Neuroscience*, *1*, 309–332.

Smith, A. T., Greenlee, M. W., Singh, K. D., Kraemer, F. M., & Hennig, J. (1998). The processing of first- and second order motion in human visual cortex assessed by functional resonance imaging (fMRI). *Journal of Neuroscience, 18*, 3816–3830.

Taylor, J. G., Schmitz, N., Ziemons, K., Grosse-Ruyken, M.-L., Gruber, O., Hueller-Gaertner, H.-W., & Shah, N. J. (2000). The network of brain areas involved in the motion aftereffect. *Neuroimage, 11*, 257–270.

Thomas, C. G., & Menon, R. S. (1998). Amplitude response and stimulus presentation frequency response of human primary visual cortex using BOLD EPI at 4 T. *Magnetic Resonance in Medicine, 40*, 203–209.

Talairach, J., & Tournoux, P. (1988). *Co-planar stereotaxic atlas of the human brain*. New York: Thieme Medical Publishers.

Tootell, R. B. H., Reppas, J. B., Kwong, K. K., Malach, R., Born, R. T., Brady, T. J., et al. (1995). Functional analysis of human MT and related visual cortical areas using magnetic resonance imaging. *Journal of Neuroscience, 15*, 3215–3230.

Tootell, R. B. H., Reppas, J. B., Dale, A. M., Look, R. B., Sereno, M. I., Malach, R., et al. (1995). Visual motion aftereffect in human cortical area MT revealed by functional magnetic resonance imaging. *Nature, 375*, 139–141.

Ullman, S. (1979). *The Interpretation of Visual Motion*. Cambridge, Mass: MIT Press.

Vanduffel, W., Fize, D., Peuskens, H., Denys, K., Sunaert, S., Todd, J. T., et al. (2002). Extracting 3D from motion: Differences in human and monkey intraparietal cortex. *Science, 298*, 413–415.

Watson, J. D. G., Myers, R., Frackowiak, R. S. J., Hajnal, J. V., Woods, R. P., Mazziotta, J. C., et al. (1993). Area V5 of the human brain: Evidence from a combined study using positron emission tomography and magnetic resonance imaging. *Cerebral Cortex, 3*, 79–94.

Wenderoth, P., Watson, J. D. G., Egan, G. F., Tochon-Danguy, H. J., & O'Keefe, G. J. (1999). Second order components of moving plaids activate extrastriate cortex: A positron emission tomography study. *Neuroimage, 9*, 227–234.

Wertheimer, M. (1912). Experimentelle Studien über das Sehen von Bewegung. *Zeitschrift für Psychologie, 61*, 161–265.

Woods, R. P., Cherry, S. R., & Mazziotta, J. C. (1992). Rapid automated algorithm for aligning and reslicing PET images. *Journal of Computer Assisted Tomography, 16*, 620–633.

Woodworth, R. S., & Schlosberg, H. (1954). *Experimental psychology*. London: Methuen.

Zeki, S., Watson, J. D. G., Lueck, C. J., Friston, K. J., Kennard, C., & Frackowiak, R. S. J. (1991). A direct demonstration of functional specialization in human visual cortex. *Journal of Neuroscience, 11*, 641–649.

Zeki, S., & Ffytche, D. H. (1998). The Riddoch syndrome: Insights into the neurobiology of conscious vision. *Brain, 121*, 25–45.

Zhu, X. H., Kim, S. G., Andersen, P., Ogawa, S., Ugurbil, K., & Chen, W. (1998). Simultaneous oxygenation and perfusion imaging study of functional activity in primary visual cortex at different visual stimulation frequency: Quantitative correlation between BOLD and CBF changes. *Magnetic Resonance in Medicine, 40*, 703–711.

Zhuo, Y., Tian, G. Z., Rao, H. Y., Wang, J. J., Meng, M., Chen, M., et al. (2003). Contributions of the visual ventral pathway to long-range apparent motion. *Science, 299*, 417–420.